ORGANOMETALLICS

Mild sp²Carbon−Oxygen Bond Activation by an Isolable Ruthenium(II) Bis(dinitrogen) Complex: Experiment and Theory

Samantha Lau,[†] Bryan Ward,[†] Xueer Zhou,[†] Andrew J. P. White,[†] Ian J. Casely,*[,‡]
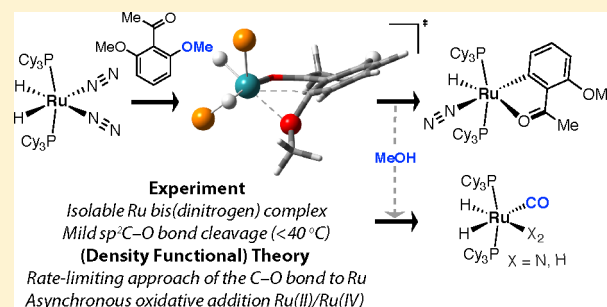Stuart A. Macgregor,*[,§] and Mark R. Crimmin*[,†]

[†]Department of Chemistry, Imperial College London, South Kensington, London SW7 2AZ, United Kingdom
[‡]Johnson Matthey Technology Centre, Blounts Court, Sonning Common, Reading RG4 9NH, United Kingdom
[§]Institute of Chemical Sciences, Heriot-Watt University, Edinburgh, EH14 4AS, United Kingdom

Ⓢ *Supporting Information*

ABSTRACT: The isolable ruthenium(II) bis(dinitrogen) complex [Ru(H)$_2$(N$_2$)$_2$(PCy$_3$)$_2$] (**1**) reacts with aryl ethers (Ar−OR, R = Me and Ar) containing a ketone directing group to effect sp²C−O bond activation at temperatures below 40 °C. DFT studies support a low-energy Ru(II)/Ru(IV) pathway for C−O bond activation: oxidative addition of the C−O bond to Ru(II) occurs in an asynchronous manner with Ru−C bond formation preceding C−O bond breaking. Alternative pathways based on a Ru(0)/Ru(II) couple are competitive but less accessible due to the high energy of the Ru(0) precursors. Both experimentally and by DFT calculations, sp²C−H bond activation is shown to be more facile than sp²C−O bond activation. The kinetic preference for C−H bond activation over C−O activation is attributed to unfavorable approach of the C−O bond toward the metal in the selectivity determining step of the reaction pathway.

Experiment
Isolable Ru bis(dinitrogen) complex
Mild sp²C−O bond cleavage (<40 °C)
(Density Functional) Theory
Rate-limiting approach of the C−O bond to Ru
*Asynchronous oxidative addition Ru(II)/Ru(IV)*

■ INTRODUCTION

The high content of elemental oxygen in the biopolymers that constitute lignocellulosic biomass has inspired chemists to develop new methods to break strong carbon−oxygen bonds.[1,2] In organometallic chemistry, a series of nickel and ruthenium precatalysts have been applied to reactions that transform carbon−oxygen bonds of ethers into carbon−hydrogen,[3,4] carbon−carbon,[5−10] or carbon−boron[11,12] bonds by hydrogenolysis, cross-coupling, or borylation, respectively.[13] Arguably as important as the synthetic advances is understanding the mechanism of C−O bond activation.

For most established catalyst systems based on nickel complexes, at least two distinct pathways for C−O bond cleavage have been proposed. While many studies invoke Ni(0)/Ni(II) catalytic cycles, oxidative addition of an sp²C−O bond of an ether to a nickel organometallic under catalytic conditions has little experimental support.[14−16] Martin and co-workers have provided experimental and theoretical backing for sp²C−O bond cleavage from a ligand-based reaction of a Ni(I) arene complex.[17]

Ruthenium hydride catalysts have been reported in elegant examples of cross-coupling reactions of aryl ethers with organoboranes.[18−22] These reactions rely on a suitable group to direct the catalyst to an adjacent bond. In many cases C−H and C−O bond functionalization are competitive. Kakiuchi and co-workers have shown that the biaryl ether represented in Figure 1 reacts with [Ru(H)$_2$(CO)(PPh$_3$)$_3$] at high temperature to give an isolable ruthenium-aryloxide product.[23] This

High-temperature C−O bond activation (*reference 23*)
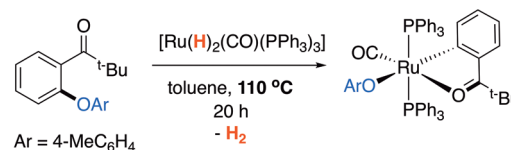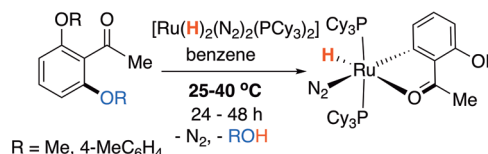

Low-temperature C−O bond activation (*this work*)

Figure 1. sp²C−O bond activation by ruthenium phosphine complexes.

reaction has been calculated to occur by oxidative addition of the C−O bond to a 16-electron ruthenium(0) complex, [Ru(PPh$_3$)$_2$(CO)(L)] (L = substrate coordinated through the directing group).[24] In related studies, Bergman and co-workers have reported ruthenium catalysts for the hydrogen-shuttling sp³C−O bond cleavage of 2-aryloxy-1-arylethanols, simple models of the β-[O]-4′ linkage of lignin. Computational data again support the involvement of a Ru(0)/Ru(II) redox couple,
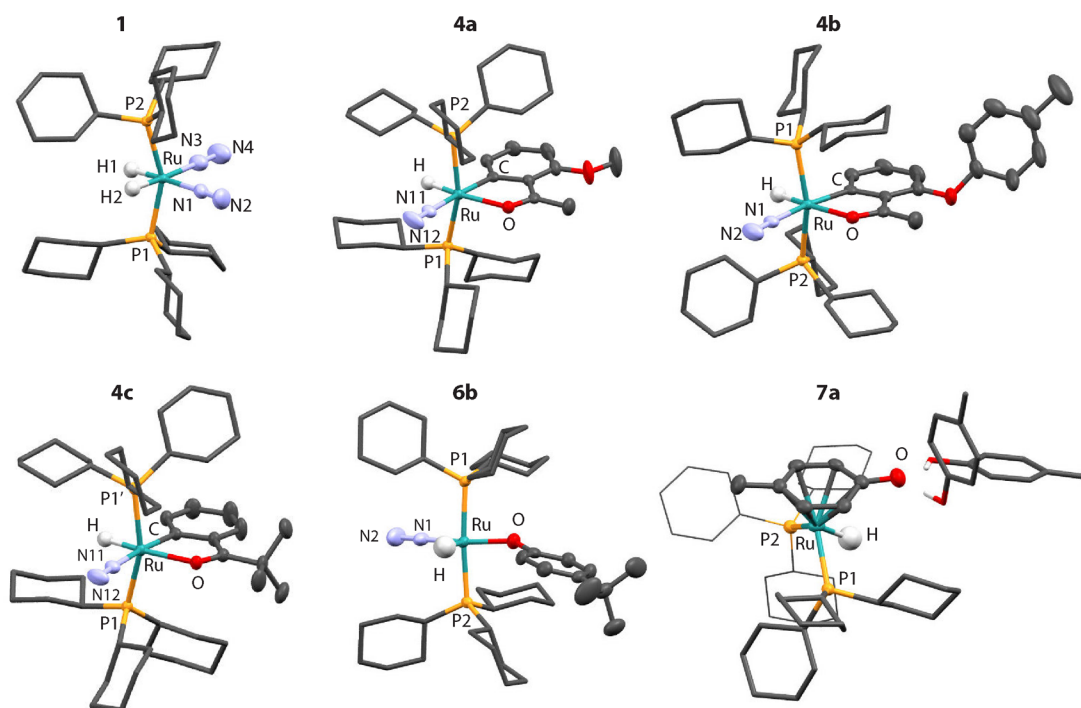
Figure 2. Crystal structures of **1**, products of C−X activation **4a−c** (X = H and O), and side products **6b** and **7a**.

and the key C−O bond breaking step is proposed to occur by oxidative addition to Ru(0).[25−27]

Here we show that [Ru(H)$_2$(N$_2$)$_2$(PCy$_3$)$_2$] (**1**), originally reported as a reactive intermediate prone to decomposition,[28] can be isolated and effects both sp^{2}C−H and sp^{2}C−O bond activation of methyl aryl and biaryl ethers under exceptionally mild conditions (25−40 °C) provided the substrate contains a suitable ketone directing group adjacent to the C−X bond (X = H and OR). We rationalize the experimental findings through an in-depth DFT analysis of the plausible pathways for C−X bond activation. We conclude that consideration of both the C−X bond breaking step and the energetics to form the reactive transition metal fragment that participates in this step is essential to compare the mechanisms of bond activation. We show that the lowest energy pathway for **1** to effect bond cleavage involves oxidative addition of the C−O bond to Ru(II).

■ EXPERIMENTAL SECTION

Full experimental details including the preparation of materials, conditions of C−X bond activation reactions, spectroscopic and crystallographic data, and details of the computational methods are given in the Supporting Information.

■ RESULTS AND DISCUSSION

Isolation of [Ru(H)$_2$(N$_2$)$_2$(PCy$_3$)$_2$] (1). Prepared from [Ru(H)$_2$(η^2-H$_2$)$_2$(PCy$_3$)$_2$],[29−31] **1** is indefinitely stable under an atmosphere of dinitrogen but subject to fast decomposition when stored under argon or placed under vacuum. During ligand exchange experiments to form **1**, [Ru(H)$_2$(η^2-H$_2$)(N$_2$)-(PCy$_3$)$_2$] was identified as an intermediate demonstrating resonances at δ −8.48 ppm and δ 68.8 ppm by ^{1}H and ^{31}P{^{1}H} NMR spectroscopy, respectively. This complex has a diffusion coefficient near-identical to that of **1** by DOSY studies. The assignment of [Ru(H)$_2$(η^2-H$_2$)(N$_2$)(PCy$_3$)$_2$] was confirmed by mixing the bis(dinitrogen) and bis(dihydrogen) complexes in a

1:1 ratio under an atmosphere of argon. Despite the discovery of [Ru(NH$_3$)$_5$(N$_2$)]$^{2+}$ initiating the field of transition metal dinitrogen chemistry,[32,33] complex **1** is the first structurally characterized bis(dinitrogen) complex of ruthenium (Figure 2, Table 1).[34,35] The single crystal data support the previous assignment of **1** as a dihydride complex with cis-disposed dinitrogen ligands.[28,36]
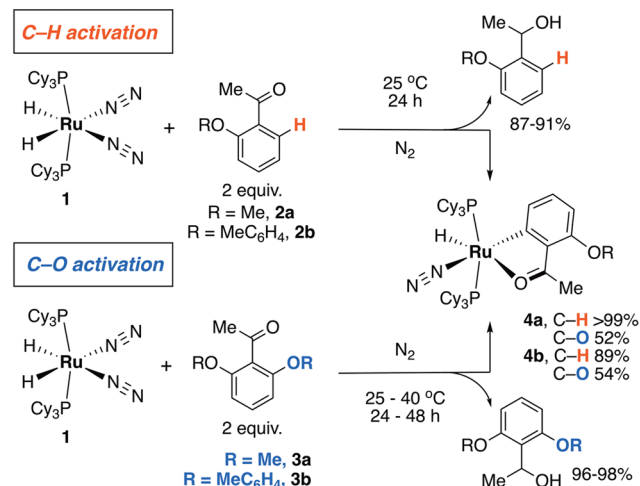
Table 1. Bond Lengths (Å) and Angles (deg) in 1 and 4a−c

|	1	4a	4b	4c
Ru−N	2.010(3) 2.013(3)	1.978(2)	1.9803(19)	1.975(2)
Ru−P	2.3382(7) 2.3392(6)	2.3529(7) 2.3542(7)	2.3562(6) 2.3571(6)	2.3459(5) 2.3460(5)
N−N	1.134(4) 1.116(3)	1.107(3)	1.105(2)	1.107(3)
Ru−C		2.034(2)	2.042(2)	2.043(3)
O−Ru−C		76.89(7)	77.35(7)	76.49(9)

Competitive C−H and C−O Bond Activation. The reaction of **1** with 2-methoxyacetophenone (**2a**) or 2-p-tolyloxyacetophenone (**2b**) in a 1:2 ratio proceeded rapidly to form the corresponding cyclometalated species, **4a−b**, formed from C−H activation of 1 equiv of substrate. This reaction is accompanied by transfer hydrogenation of the second equivalent of substrate.[37] Using a 1:1 ratio of reagents, the same result is observed but with half of **1** unconsumed. Addition of **1** to 2,6-dimethoxyacetophenone (**3a**) resulted in facile C−O bond activation, again producing **4a** as the predominant ruthenium-containing product. Similar results were obtained using biaryl ether **3b** to form complex **4b**. Hence, **1** is capable of cleaving both sp^{2}C−OMe and sp^{2}C−OAr bonds below 40 °C, and both reactions proceed slowly at room temperature (Scheme 1). The Ru-containing side

products of C−O bond cleavage are represented in Scheme 1, and their formation is detailed below.

Scheme 1. sp²C−O and sp²C−H Bond Activation of Methyl Aryl and Biaryl Ethers with 1 and Key Side Products Formed from C−O Activation
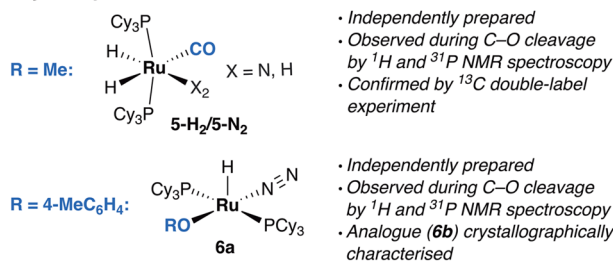

The propensity of $[Ru(H)_2(\eta^2\text{-}H_2)_2(PCy_3)_2]$ to effect the cyclometalation[38] and catalytic functionalization[39−41] of the sp²C−H bond of aromatic substrates containing a suitable directing group is well-established, but there is no precedent for C−O bond activation with this complex. Control reactions show that C−O bond activation is sensitive to the nature of the ligands on ruthenium (N_2 versus H_2) and the atmosphere under which the reaction is conducted. Reaction of 1 with 3a under argon proceeded to give 4a over 5 h, while that under N_2 required 24 h to reach completion, more accurately, $t_{1/2}(N_2) = 6.0$ h and $t_{1/2}(Ar) = 1.6$ h. Reaction of 3a with $[Ru(H)_2(\eta^2\text{-}H_2)_2(PCy_3)_2]$ under an atmosphere of H_2 fails to result in C−O cleavage with transfer hydrogenation of the ketone observed regardless of the reaction stoichiometry. In combination, the experiments show that a labile N_2 ligand on ruthenium is necessary for C−O activation; indeed, exogenous N_2 inhibits the rate of this reaction.

Complexes 4a and 4b were characterized by distinctive triplets in the hydride region of the ^1H NMR spectrum at δ −14.89 (t, $^2J_{P-H} = 24.5$ Hz) and −14.82 (t, $^2J_{P-H} = 24.1$ Hz) ppm, respectively, along with near-identical $^{31}P\{^1H\}$ resonances (4a, δ 39.1 ppm; 4b, δ 39.9 ppm). While ultimately resolved by X-ray diffraction studies (Figure 2), the retention of the dinitrogen ligand on ruthenium was supported by infrared absorptions for both Ru−H (4a, 1964 cm⁻¹; 4b, 1983 cm⁻¹) and N≡N bonds (4a, 2078 cm⁻¹; 4b, 2106 cm⁻¹). The ruthenium-bound carbon atoms of the cyclometalated ligands

were observed in the expected region of the ^{13}C NMR spectrum and correlated with the Ru−H resonance by HMBC experiments (4a, δ 212.2 ppm; 4b, δ 211.8 ppm).

In the case of substrates 2a−b, despite the presence of both *ortho* C−H and C−O bonds, exclusive C−H activation was observed. Similarly, an intermolecular competition experiment in which 1 was reacted with 2 equiv of 3a and 2 equiv of 2,2-dimethylpropiophenone led to exclusive formation of C−H activation product 4c (Scheme 2). Attempts failed to extend the scope of the C−O cleavage reaction to substrates that did not contain a suitable directing group such as anisole or benzyl phenyl ether.

Scheme 2. Intermolecular Competition Experiment between sp²C−O and sp²C−H Bond Activation
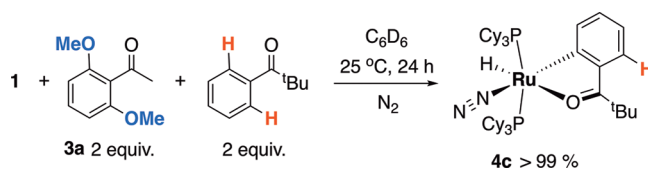

It is notable that although both C−O cleavage reactions proceed to give organometallics in approximately 50% yield neither contain the −OR fragment from the broken C−OR bond. Furthermore, transfer hydrogenation of the organic substrates occurs in both C−H and C−O activation reactions. These data raise a number of questions: What is the destination of the −OMe and −OAr groups following C−O bond cleavage? What is the source of dihydrogen for the transfer hydrogenation? Is transfer hydrogenation required to generate a reactive Ru-complex capable of effecting C−O bond cleavage?

Ru-Containing Side Products from C−O Activation. We hypothesized that the initial side products of C−O bond activation are the alcohols, methanol (from 3a), and 4-methyl phenol (from 3b) that go on to react with 1 at a faster rate than the ethers themselves. In line with literature findings, methanol reacts rapidly with 1 to form an equilibrium mixture of 5-N_2/5-H_2 (Scheme 3a).[28,42] These ruthenium carbonyl complexes are formed during reactions of the methyl ether 3a with 1 in ~30% yield as evidenced by $^{31}P\{^1H\}$ and ^1H NMR spectroscopy. Additional evidence for the formation of a metal carbonyl under C−O cleavage conditions was provided by the reaction of 1 with double ^{13}C-labeled 2,6-dimethoxyacetophenone. Following the reaction by ^{13}C NMR spectroscopy revealed the formation of a new metal carbonyl characterized by a diagnostic resonance at δ 204.5 ppm (Scheme 3b). In combination, these experiments provide compelling evidence for the formation of a Ru−methoxide intermediate that readily decomposes to a metal carbonyl. For comparison, nickel alkoxide intermediates are prone to β-hydride elimination,[43,44] and the formation of nickel carbonyl complexes has been reported during reactions that break strong C−O bonds of methyl aryl ethers.[17,43]

Monitoring the reaction of 1 with 4-methyl (or 4-*tert*-butyl) phenol as a function of time revealed the formation of a mixture of 6−8 prior to workup (Scheme 4).[45] The structural assignment was confirmed by a combination of $^{31}P\{^1H\}$ and ^1H NMR spectroscopy (including VT and 2D experiments) and X-ray crystallography. These experiments included the isolation and separation of 6b, an analogue of 6a which proved amenable to purification by fractional crystallization.

Scheme 3
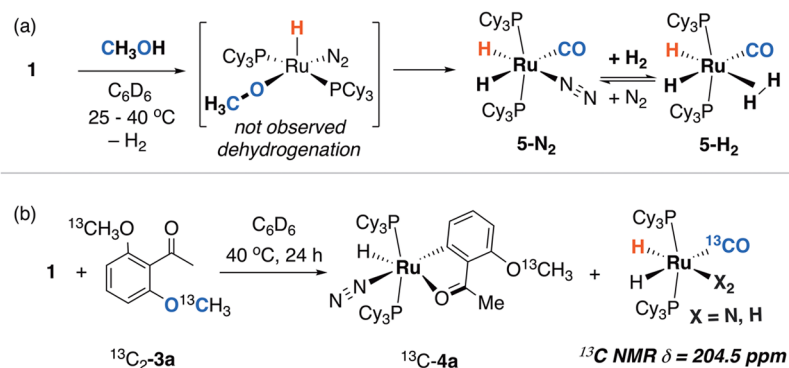
[a]Side products from C−O bond activation of **3a**. [b]Side products from reaction of [13]C-**3a** with **1**.

Scheme 4. Side Products from C−O Bond Activation of 3b
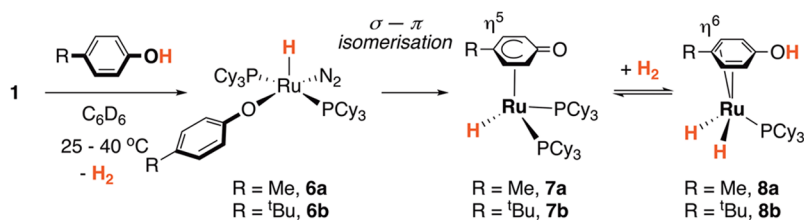
Square-based pyramidal ruthenium-aryloxide complex **6a** is the major side product observed in the C−O cleavage reaction of **3b** (~20% yield). This complex is characterized by a diagnostic resonance at δ 41.9 ppm in the $^{31}P\{^1H\}$ NMR spectrum and a heavily shielded hydride resonance at δ −25.86 (t, J = 19.2 Hz) ppm in the ^1H NMR data. Complexes **7a** and **8a** are also both observed during C−O bond activation of **3b** with **1**, albeit in smaller amounts than **6a**, and are minor side products of this reaction (~5% combined yield).

While analogous reactions between Ru(II) hydrides and phenols have been reported previously, there is a dearth of single crystal X-ray studies to support the proposed structures of the reaction products.[46]

Complex **6b** contains, to the best of our knowledge, the first structurally characterized *trans*-relation (O−Ru−N = 166.22(10)°) between a σ-aryloxide and dinitrogen ligand (Figure 2). Both the Ru−O bond length (2.0181(18) Å) and the Ru−N bond length (1.878(2) Å) are short. For comparison, the former distance can be compared to the range found in σ-phenoxide complexes (2.108(6)−2.152(2) Å) and the latter to **4a**−**c** (1.975(2)−1.9803(19) Å).[45−48] These data are a reflection of the weaker *trans*-influence of the σ-aryloxide in comparison to the σ-aryl ligand[47] and the π-basicity of the aryloxide increasing back-donation to the dinitrogen ligand. For comparison, *trans*-disposed ether and dinitrogen ligands in a monomeric ruthenium complex have M−O and M−N bond lengths of 2.117(3) and 1.946(3) Å, respectively.[49−51]

Transfer Hydrogenation of the Ketone. Monitoring the C−X bond activation reactions as a function of time revealed that transfer hydrogenation of the ketone does not precede bond activation but rather occurs at the same time. Esteruelas and co-workers have also observed substrate hydrogenation during C−H bond activation of ketones promoted by ruthenium POP−pincer complexes.[52] Transfer hydrogenation of the first equiv of substrate with **1** could be a potential route

to generate coordinatively unsaturated Ru(0) complexes. These latter species have been suggested by DFT to play an important role in C−O and C−H bond activation and will be considered as potential intermediates in the key bond breaking events in the computational studies below (see "Plausible Pathways for C−O Activation").

An alternative explanation for the observed transfer hydrogenation process is that **1** (or related species) could catalyze the hydrogenation of the substrate. The H₂ required is potentially liberated during the C−X bond activation reactions. In the case of C−H activation, H₂ is formed from the breaking C−H and Ru−H bonds, while in the case of C−OR activation, H₂ is generated by either dehydrogenation of the methoxide ligand to form the carbonyl complex **5-N₂**/**5-H₂** (R = Me) or during generation of the aryloxide **6a** (R = Ar).

Summary of Experimental Findings. In combination, the experimental data show the following: (i) Facile C−O activation of aryl and methyl ethers occurs with the ruthenium(II) complex **1** below 40 °C provided the substrate contains a suitable directing group. (ii) The initial side products of C−O bond activation are ruthenium−alkoxide/aryloxide complexes. (iii) C−O bond activation can be inhibited by addition of exogenous dinitrogen. (iv) C−H activation occurs at a faster rate than C−O bond activation. The computational studies presented below will rationalize these experimental data.

Computational Studies. Potential reaction mechanisms were studied by DFT using the Gaussian 09 suite and optimizations employed the BP86 functional.[53−55] Ru and P centers were described with Stuttgart RECPs and associated basis sets (ECP28MWB for Ru and ECP10MWB for P).[56−58] The P basis set was augmented with the addition of d-orbital polarization (ζ = 0.387).[59] 6-31+G* basis sets were used for N and O, and 6-31G** basis sets were used for all other atoms.[60−62] Free energies are corrected for both benzene solvent (PCM approach) and dispersion effects (Grimme's D3 parameter set with Becke−Johnson (BJ) damping).[63,64] Full

details of the computational methods are provided in the Supporting Information.

Plausible Pathways for C−O Activation. In analyzing plausible mechanisms of C−O bond activation from **1** we need to consider both the key bond breaking step and the energetics to form the reactive transition metal fragment that participates in this step. Let us consider a series of plausible processes for C−O bond cleavage, namely, (i) oxidative addition of the C−O bond to Ru(0), (ii) hydrodeoxygenation by hydride attack on the C−O bond of the Ru(II) coordinated substrate, and (iii) oxidative addition of the C−O bond to Ru(II) (Scheme 5).

Scheme 5. Plausible Mechanisms for C−O Activation
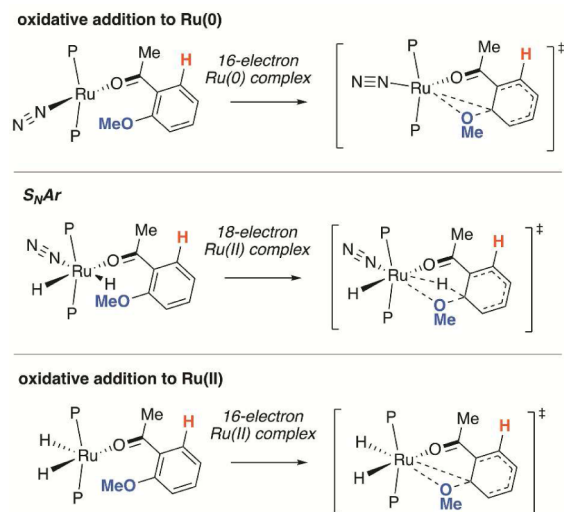
Oxidative addition of C−O bonds of ethers to Ru(0) carbonyl complexes has been widely invoked in Ru-catalyzed cross-coupling reactions of ethers with boronic esters.[18−22] Lin and co-workers have recently calculated a low-energy transition state for the oxidative addition of a C−O bond to the square-planar 16-electron complex *trans*-[Ru(PPh$_3$)$_2$(CO)(L)].[24] Directing-group-assisted C−H activation has been calculated to occur by similarly facile Ru(0)/Ru(II) redox process.[65,66] While the Ru(0)/Ru(II) mechanisms for C−X bond activation are becoming generally accepted, the following question remains: What are the barriers to generate the reactive 16-electron fragments from the Ru(II) precursors employed in experiments?

The results of the calculations that address this question for **1** are summarized graphically alongside the highest energy transition states for the C−O activation step in Figure 3. The data are presented in detail in Figures S27−31. Although oxidative addition of a C−O bond to Ru(0) is facile, formation of the required 16-electron intermediate is kinetically challenging. This species could be generated by either reductive elimination of H$_2$ from **1** or transfer hydrogenation of a further equivalent of the ketone substrate (as observed experimentally). The highest transition states for these processes reach 32−38 kcal mol^{-1}. In contrast, ligand exchange reactions that give rise to intermediates capable of C−O bond activation at Ru(II) are lower in energy, <30 kcal mol^{-1}. Two pathways for C−O bond activation are plausible from these Ru(II) intermediates (hydrodeoxygenation or oxidative addition), and both have transitions states that are similar to or lower than those required to form the 16-electron Ru(0) species from **1**. The transition state for the S$_N$Ar path for C−O bond activation by hydrodeoxygenation,[67−69] is 1.8 kcal mol^{-1} higher than the barrier involving oxidative addition of the C−O bond to Ru(II) to form Ru(IV).

To assess the possibility of a functional dependency effect on competing pathways, we recomputed key intermediates and transition states involved with a range of different functionals (Table S2). The relative energy barriers were reproduced consistently for each of the functionals and the Ru(II)/Ru(IV) pathway was consistently found to be the most favorable pathway of those examined. The results therefore indicate an independence from functional influence.

The data suggest that while a number of pathways for C−O bond activation are potentially competitive the oxidative addition of the C−O bond to Ru(0) is the least accessible due to the high barriers to form the required intermediate. In the remainder of this manuscript, we provide a detailed analysis of the lowest energy mechanism for C−O bond activation, which involves changes in oxidative state between Ru(II) and Ru(IV). We compare the pathways for C−O and C−H cleavage that derive from common intermediates.

C−H Activation. Clot and co-workers have previously calculated the C−H activation of acetophenone by [Ru-(H)$_2$(η^2-H$_2$)$_2$(PMe$_3$)$_2$] and concluded that following displacement of 2 equiv of H$_2$ by the ketone and formation of an agostic complex the reaction proceeds by a σ-complex assisted
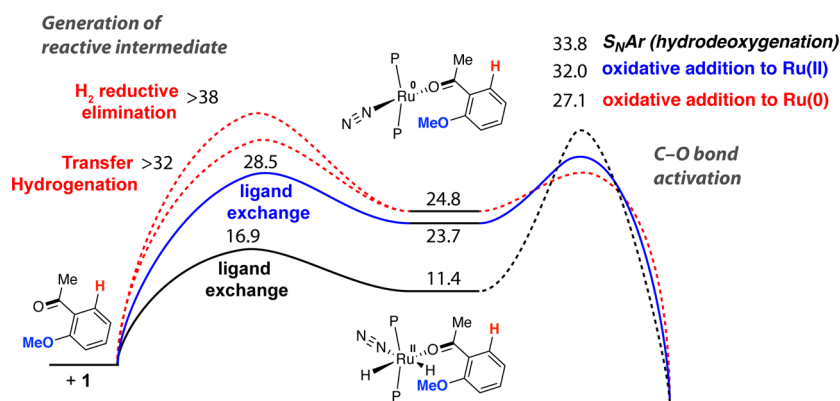

Figure 3. Comparison of the highest energy transition states for TM fragment generation and C−O activation. Gibbs free energies in kcal mol^{-1}. P = PCy$_3$.
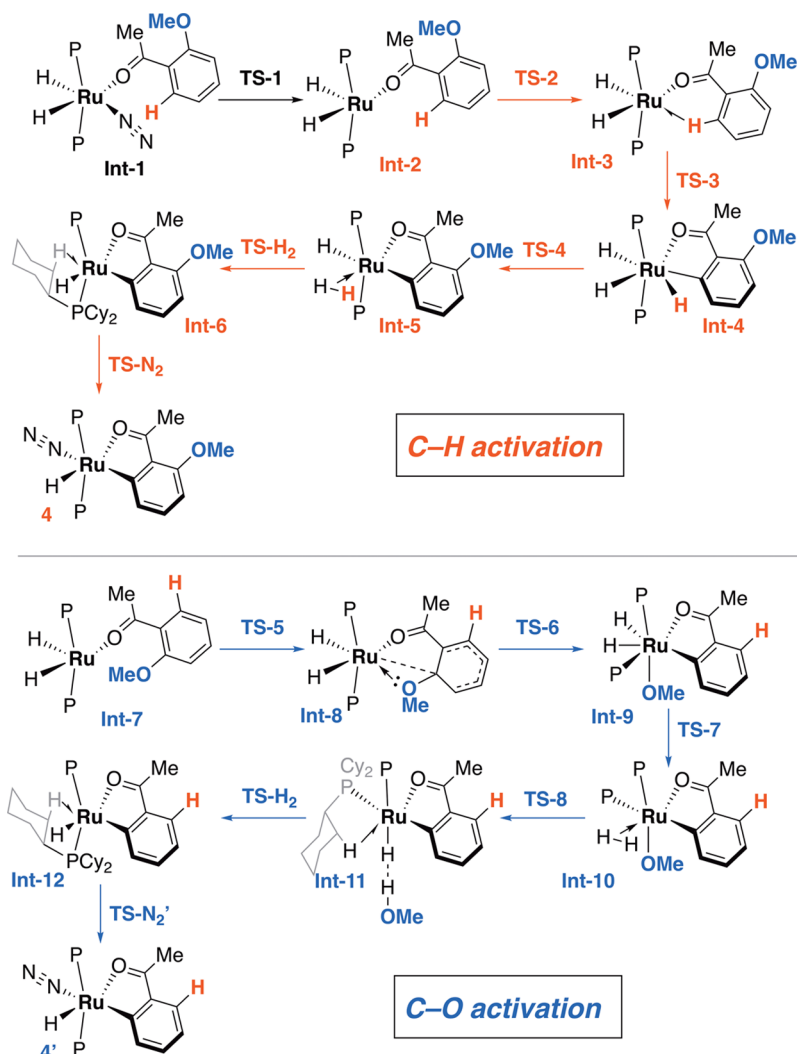
Figure 4. Structures of stationary points in C−H and C−O activation by **1**.
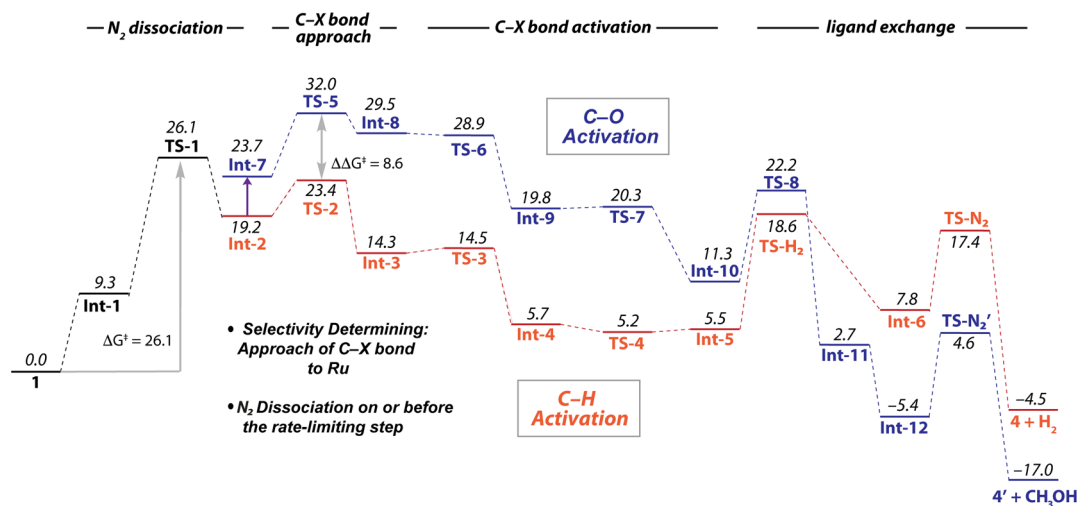

Figure 5. Calculated pathways for C−H (red) and C−O (blue) activation. Gibbs free energies in kcal mol^{-1}; liberated N$_2$ not shown.

metathesis (σ-CAM)-like mechanism.[70,71] Importantly, this study demonstrated that the directing-group-assisted pathway was considerably lower in energy than those which did not involve coordination of the carbonyl group to ruthenium. In the

current case, while modification of the substrate to **2a** and ruthenium precursor to **1** produces a near-identical low-energy reaction pathway for the C−H bond cleavage step, considering the steps prior to coordination of the C−H bond has identified
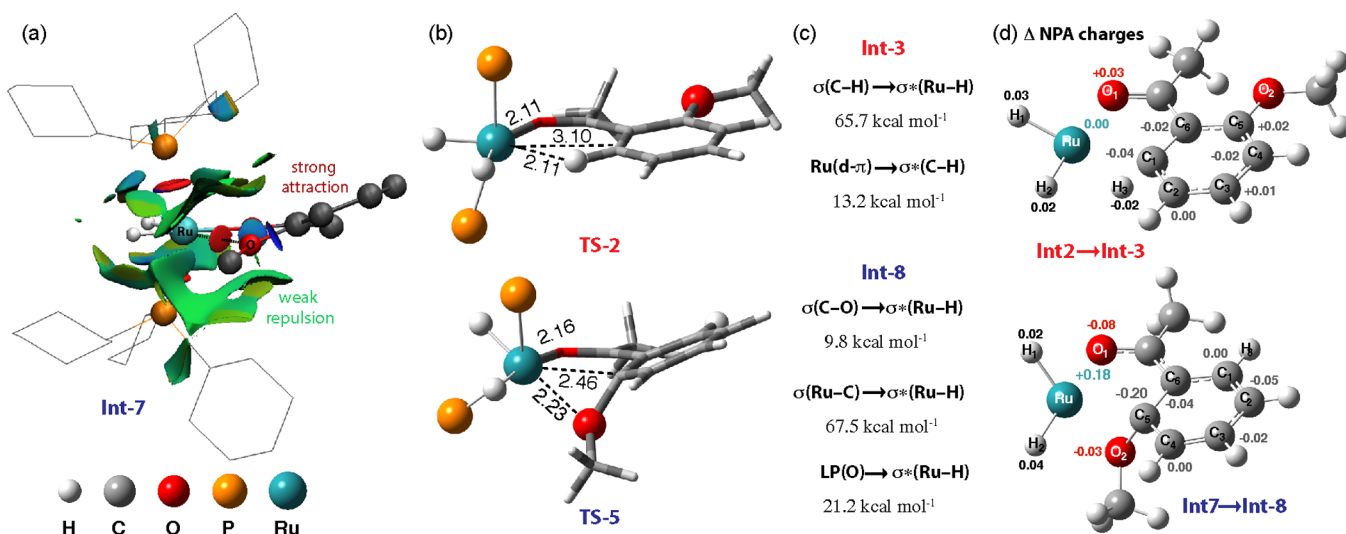
Figure 6. (a) NCI plot of **Int-7** showing the key repulsive noncovalent interaction. (b) Molecular models of **TS-2** and **TS-5** with selected bond lengths (Å). (c) Selected NBO second-order perturbation analysis data on **Int-3** and **Int-8**. (d) NBO analysis showing the difference in the NPA charges between **Int-3/Int-2** and **Int-7/Int-8**.

further important features of this reaction (Figures 4 and 5). Stepwise dissociation of 2 equiv of N$_2$ from **1** with formation of the five-coordinate intermediate **Int-2** is endergonic, $\Delta G° = +19.2$ kcal mol^{-1}, and provides the highest energy transition state (**TS-1**) on the potential energy surface, $\Delta G^{\ddagger} = 26.1$ kcal mol^{-1} (Figure 3, blue curve).

N$_2$ dissociation from **Int-1** can therefore be considered as the rate-limiting step for C−H activation. Bond breaking and bond making processes from **Int-2** are facile. The highest transition state in C−H bond breaking from **Int-2** is **TS-2**, the approach of the C−H bond to ruthenium to form the agostic complex **Int-3** with $\Delta G^{\ddagger} = 4.2$ kcal mol^{-1}. The C−H bond cleavage transition state, **TS-3**, is only 0.2 kcal mol^{-1} higher in energy than **Int-3**, and C−H bond cleavage is rapidly followed by H−H bond formation along a flat potential energy surface on which the ruthenium(II) complex **Int-5** is the lowest energy minimum.[72] The reorganization of hydrogen atoms within the equatorial plane of ruthenium(II) complexes is well-known to proceed through low-energy, almost barrierless steps,[38,73] and related fluxional exchange process have been proposed to be facilitated by nascent H···H−H bond formation in the ground state due to donation from the σ-(M−H) orbital to the σ*-(H−H) orbital.[74,75] Dissociative exchange of H$_2$ in **Int-5** for N$_2$ forms intermediate **Int-6** and ultimately gives experimentally isolated C−H activation product **4**.

As previously concluded by Clot and co-workers, **TS-3** could be assigned as a stationary point with significant ruthenium(IV) character.[70] Moreover, in the current study **Int-4** was identified as the minimum that is directly connected to **TS-3**.[76] QTAIM and NBO calculations support the formulation of **Int-4** as a ruthenium(IV) trihydrido complex (Figure S32). A number of Ru(IV) hydrido complexes are known,[75,77] and Sabo-Etienne and co-workers have recently characterized a Ru(IV) hydridotrisilyl complex of the form [RuH(SiR$_3$)$_3$L$_3$] by neutron diffraction.[78] Relaxed scan calculations along this potential energy surface did not allow the identification of a concerted C−H bond breaking and H−H bond forming process.

C−O Activation. Considering the analogous pathway for C−O bond activation, the transition state for the approach of the C−O bond toward ruthenium, **TS-5**, is higher in energy than

TS-2 on the C−H activation pathway. This is therefore the selectivity-determining step. Once **Int-8** is formed, C−O activation, like C−H activation, is facile and results in the generation of Ru(IV) intermediate **Int-9** at $+19.8$ kcal mol^{-1}. Formation of H$_2$ from **Int-9** via **TS-7** generates the Ru(II) complex, **Int-10**.

As with C−H activation, the bond breaking and making processes that occur from **Int-7** to **Int-10** connect two Ru(II) complexes by Ru(IV) stationary points. In contrast to the C−H activation σ-CAM mechanism (in which the H from the C−H bond effectively transfers directly on to the neighboring hydride to form H$_2$), as the C−OMe bond breaks, a new H−OMe bond does not form directly. Instead, addition of the C−O bond to Ru(II) occurs in concert with the reductive coupling of the two hydride ligands already present, and this serves to re-establish the Ru(II) oxidation state in **Int-10**. The nature of the C−X bond breaking step in this pathway is subtly different to C−H activation (*vide infra*). Methanol formation proceeds from **Int-10** through **TS-8**, breaking the H−H and Ru−OMe bonds while simultaneously forming H−OMe and H−Ru bonds to generate **Int-11**. Cundari, Gunnoe, and co-workers have characterized related processes which involve the addition of H$_2$ (or C−H bonds) across Ru−OH and Ru−NH$_2$ bonds.[79,80] Methanol remains bound to the outer sphere of the ruthenium complex in **Int-11** through a dihydrogen bond (1.59 Å), whereas the vacant site at Ru is stabilized through a C−H agostic interaction from a tricyclohexylphosphine ligand (Figure S34). Dissociation of methanol is facile, leaving the five coordinate complex, **Int-11**, with *cis*-phosphine ligands (Figures 4 and 5). Due to the ease of the ligand reorganization processes, **Int-11** can undergo an intramolecular isomerization. Swinging of a phosphine from an equatorial to axial site yields **Int-12**, which retains a C−H agostic interaction, and readily coordinates dinitrogen forming the reaction products (Figure S35). Several pathways were characterized for product formation from **Int-9** but that shown in Figures 4 and 5 was the most accessible.[81] Dehydrogenation of CH$_3$OH to form **5-N$_2$/5-H$_2$** by **1** was also investigated computationally. Formation of the carbonyl complexes occurs through well-understood β-hydride elimination and C−H activation steps all of which are

computed to be more accessible than the preceding C−O activation (Figure S38).[82,83]

Selectivity Determining Approach of the C−X Bond to Ruthenium. Comparison of **TS-2** and **TS-5** explains the experimentally observed selectivity. The free energy barrier for C−H activation is considerably lower than C−O activation ($\Delta\Delta G$ = 8.6 kcal mol^{-1}). Approach of the C−O bond toward ruthenium is less favored than that of the C−H bond due to a combination of repulsive noncovalent interactions forcing ligand reorganization. The importance of repulsive interactions between substrates and transition metals has long been argued when modeling reactions that break strong C−F bonds.[84,85] NBO charge analysis highlights negative charge accumulation at both Ru and O(Me) in **TS-5**. In contrast, the Ru($d\pi$)···C−H(σ) repulsion is less significant. Consequently, as the C−O bond approaches Ru, the acetophenone aryl ring is twisted out of the equatorial plane in **TS-5** as Ru interacts preferentially with the *ipso*-carbon (*vide infra*). The structural reorganization that is forced by distortion of the substrate is facilitated by the flexibility of the coordinated phosphine ligands (Figure 6b). The P−Ru−P angle in **TS-5** of 132° is ∼30° smaller than that in **TS-2** (Table S3). The phosphine ligands are ultimately forced into a *cis*-like geometry in **Int-9**. It is clear despite the energetic penalty that accompanies the structural distortion that the elasticity of the P−Ru−P angle is important for C−O cleavage. A number of relevant ruthenium complexes with *cis*-disposed PCy$_3$ ligands are known.[86−88]

Breaking of the C−X Bond. Both bond activation steps involve oxidative addition of the C−X bond to Ru(II). There are, however, subtle differences between the C−H and C−O cleavage mechanisms. As both pathways contain an early transition state for C−X bond activation, comparison of **Int-3** and **Int-8** elucidates the key differences. Second-order perturbation analysis allows **Int-3** to be classified as a typical agostic complex. Donation from the σ-(C−H) orbital to the σ^*-(Ru−H) is accompanied by back-donation from a filled d-orbital of Ru to the σ^*-(C−H) (Figure 6c). NBO calculations show that formation of this agostic complex from **Int-2** occurs with only minor perturbation of the electron density at the Ru and C centers (Figure 5d). It can be concluded that C−H bond breaking occurs by population of the σ^*-(C−H) orbital with electrons from Ru and formation of a Ru(IV) organometallic.

In contrast, formation of **Int-8** from **Int-7** on the C−O activation pathway occurs with pyramidalization at the *ipso*-carbon of the aromatic ring and accumulation of charge at both this site and, to a lesser extent, the *ortho*- and *para*-positions. Concurrently the Ru center undergoes charge depletion (Figure 6d). While QTAIM analysis shows bond critical paths between Ru−C, C−O, and O−Ru in this intermediate, second-order perturbation analysis from the NBO calculations suggests that it cannot be simply described as a σ-complex (Figure S40). No significant donation nor back-donation to or from the σ-(C−O) bond is calculated (Figure 6). Moreover the small positive $\nabla^2\rho_b$ and negative H_b values at the bond critical points between Ru and C from the QTAIM data indicate the formation of a partially covalent bond. In combination the data suggest an asynchronous pathway for C−O bond activation in which Ru−C bond formation precedes Ru−O bond formation. This bond breaking/bond making event is reminiscent of nucleophilic aromatic substitution. Attack of the metal-based nucleophile on the aromatic ring is followed by transfer of the methoxy group to the forming Ru(IV) center.

CONCLUSIONS

A comprehensive study of the organometallic products of the sp^{2}C−O bond activation of aryl methyl and biaryl ethers bearing ketone directing groups by $[Ru(H)_2(N_2)_2(PCy_3)_2]$ has been presented. Significant quantities of ruthenium-aryloxide or ruthenium−carbonyl side products are formed during C−O cleavage and their formation is rationalized based on the initial formation of alcohol byproducts that react with $[Ru(H)_2(N_2)_2(PCy_3)_2]$ at a faster rate than the ethers. In substrates where an ortho C−H bond is available there is a kinetic preference for C−H over C−O bond activation.

DFT studies revealed that the lowest energy pathway for bond activation involves the oxidative addition of the C−X bond to Ru(II) to form Ru(IV) intermediates. In this pathway, the approach of the C−X bond to Ru is selectivity determining. Ligand dissociation, i.e., N$_2$ dissociation, occurs en route to the rate-determining step, and stationary points along the C−O cleavage pathway require large changes in the P−Ru−P angle. Alternative pathways for C−O bond activation were explored and shown to be less favorable due to high-energy transition states for either the bond activation step (S$_N$Ar/hydrodeoxygenation) or the formation of the reactive intermediates required for bond activation (oxidative addition to Ru(0)). The discovery of a ruthenium(II) complex capable of C−O bond activation under mild conditions (25−40 °C) and the new Ru(II)/Ru(IV) mechanism we present for C−O bond cleavage may have broad implications for the development of new catalysts for chemical transformation of renewable resources.

ASSOCIATED CONTENT

⑤ Supporting Information

Editable NMR data and coordinate files are available via a repository maintained by Imperial College London (DOI: 10.14469/hpc/2100). The Supporting Information is available free of charge on the ACS Publications website at DOI: 10.1021/acs.organomet.7b00632.

> Experimental procedures, details of the DFT studies, single crystal X-ray data, and multinuclear NMR spectra (PDF)
> Cartesian coordinates (XYZ)

Accession Codes

CCDC 1530724−1530730 contain the supplementary crystallographic data for this paper. These data can be obtained free of charge via www.ccdc.cam.ac.uk/data_request/cif, or by emailing data_request@ccdc.cam.ac.uk, or by contacting The Cambridge Crystallographic Data Centre, 12 Union Road, Cambridge CB2 1EZ, UK; fax: +44 1223 336033.

AUTHOR INFORMATION

Corresponding Authors

*E-mail: m.crimmin@imperial.ac.uk.
*E-mail: s.a.macgregor@hw.ac.uk.
*E-mail: ian.casely@matthey.com.

ORCID ⊙

Bryan Ward: 0000-0002-1744-4930
Stuart A. Macgregor: 0000-0003-3454-6776
Mark R. Crimmin: 0000-0002-9339-9182

Author Contributions

S.L. and B.W. contributed equally to the creation of this work.

Notes

The authors declare no competing financial interest.

■ REFERENCES

(1) Ragauskas, A. J.; Williams, C. K.; Davison, B. H.; Britovsek, G.; Cairney, J.; Eckert, C. A.; Frederick, W. J., Jr; Hallett, J. P.; Leak, D. J.; Liotta, C. L.; Mielenz, J. R.; Murphey, R.; Templer, R.; Tschaplinski, T. *Science* **2006**, *311*, 484−489.

(2) Kärkäs, M. D.; Matsuura, B. S.; Monos, T. M.; Magallanes, G.; Stephenson, C. R. J. *Org. Biomol. Chem.* **2016**, *14*, 1853−1914.

(3) Atesin, A. C.; Ray, N. A.; Stair, P. C.; Marks, T. J. *J. Am. Chem. Soc.* **2012**, *134*, 14682−14685.

(4) Sergeev, A. G.; Hartwig, J. F. *Science* **2011**, *332*, 439−443.

(5) Yonova, I. M.; Johnson, A. G.; Osborne, C. A.; Moore, C. E.; Morrissette, N. S.; Jarvo, E. R. *Angew. Chem., Int. Ed.* **2014**, *53*, 2422−2427.

(6) Cornella, J.; Martin, R. *Org. Lett.* **2013**, *15*, 6298−6301.

(7) Wang, C.; Ozaki, T.; Takita, R.; Uchiyama, M. *Chem. - Eur. J.* **2012**, *18*, 3482−3485.

(8) Wenkert, E.; Michelotti, E. L.; Swindell, C. S. *J. Am. Chem. Soc.* **1979**, *101*, 2246−2247.

(9) Rosen, B. M.; Quasdorf, K. W.; Wilson, D. A.; Zhang, N.; Resmerita, A.-M.; Garg, N. K.; Percec, V. *Chem. Rev.* **2011**, *111*, 1346−1416.

(10) Tobisu, M.; Chatani, N. *Acc. Chem. Res.* **2015**, *48*, 1717−1726.

(11) Zarate, C.; Manzano, R.; Martin, R. *J. Am. Chem. Soc.* **2015**, *137*, 6754−6757.

(12) Kinuta, H.; Tobisu, M.; Chatani, N. *J. Am. Chem. Soc.* **2015**, *137*, 1593−1600.

(13) Cornella, J.; Zarate, C.; Martin, R. *Chem. Soc. Rev.* **2014**, *43*, 8081−8097.

(14) Ogawa, H.; Minami, H.; Ozaki, T.; Komagawa, S.; Wang, C.; Uchiyama, M. *Chem. - Eur. J.* **2015**, *21*, 13904−13908.

(15) Li, Z.; Zhang, S.-L.; Fu, Y.; Guo, Q.-X.; Liu, L. *J. Am. Chem. Soc.* **2009**, *131*, 8815−8823.

(16) Xu, L.; Chung, L. W.; Wu, Y.-D. *ACS Catal.* **2016**, *6*, 483−493.

(17) Cornella, J.; Gómez-Bengoa, E.; Martin, R. *J. Am. Chem. Soc.* **2013**, *135*, 1997−2009.

(18) Kondo, H.; Akiba, N.; Kochi, T.; Kakiuchi, F. *Angew. Chem., Int. Ed.* **2015**, *54*, 9293−9297.

(19) Kakiuchi, F.; Usui, M.; Ueno, S.; Chatani, N.; Murai, S. *J. Am. Chem. Soc.* **2004**, *126*, 2706−2707.

(20) Zhao, Y.; Snieckus, V. *Chem. Commun.* **2016**, *52*, 1681−1684.

(21) Zhao, Y.; Snieckus, V. *J. Am. Chem. Soc.* **2014**, *136*, 11224−11227.

(22) Zhao, Y.; Snieckus, V. *Org. Lett.* **2015**, *17*, 4674−4677.

(23) Ueno, S.; Mizushima, E.; Chatani, N.; Kakiuchi, F. *J. Am. Chem. Soc.* **2006**, *128*, 16516−16517.

(24) Wang, Z.; Zhou, Y.; Lam, W. H.; Lin, Z. *Organometallics* **2017**, *36*, 2354−2363.

(25) Nichols, J. M.; Bishop, L. M.; Bergman, R. G.; Ellman, J. A. *J. Am. Chem. Soc.* **2010**, *132*, 12554−12555.

(26) Wu, A.; Patrick, B. O.; Chung, E.; James, B. R. *Dalton Trans.* **2012**, *41*, 11093−11106.

(27) Chmely, S. C.; Kim, S.; Ciesielski, P. N.; Jiménez-Osés, G.; Paton, R. S.; Beckham, G. T. *ACS Catal.* **2013**, *3*, 963−974.

(28) Christ, M. L.; Sabo-Etienne, S.; Chung, G.; Chaudret, B. *Inorg. Chem.* **1994**, *33*, 5316−5319.

(29) Alcaraz, G.; Grellier, M.; Sabo-Etienne, S. *Acc. Chem. Res.* **2009**, *42*, 1640−1649.

(30) Arliguie, T.; Chaudret, B.; Morris, R. H.; Sella, A. *Inorg. Chem.* **1988**, *27*, 598−599.

(31) Chaudret, B.; Poilblanc, R. *Organometallics* **1985**, *4*, 1722−1726.

(32) Allen, A. D.; Senoff, C. V. *Chem. Commun. (London)* **1965**, 621−622.

(33) Senoff, C. V. *J. Chem. Educ.* **1990**, *67*, 368−370.

(34) Abdur-Rashid, K.; Gusev, D. G.; Lough, A. J.; Morris, R. H. *Organometallics* **2000**, *19*, 1652−1660.

(35) Gusev, D. G.; Dolgushin, F. M.; Antipin, M. Y. *Organometallics* **2000**, *19*, 3429−3434.

(36) Ben Said, R.; Hussein, K.; Tangour, B.; Sabo-Etienne, S.; Barthelat, J.-C. *J. Organomet. Chem.* **2003**, *673*, 56−66.

(37) Linn, J. D. E.; Halpern, J. *J. Am. Chem. Soc.* **1987**, *109*, 2969−2974.

(38) Toner, A. J.; Gründemann, S.; Clot, E.; Limbach, H.-H.; Donnadieu, B.; Sabo-Etienne, S.; Chaudret, B. *J. Am. Chem. Soc.* **2000**, *122*, 6777−6778.

(39) Guari, Y.; Sabo-Etienne, S.; Chaudret, B. *J. Am. Chem. Soc.* **1998**, *120*, 4228−4229.

(40) Grellier, M.; Vendier, L.; Chaudret, B.; Albinati, A.; Rizzato, S.; Mason, S.; Sabo-Etienne, S. *J. Am. Chem. Soc.* **2005**, *127*, 17592−17593.

(41) Guari, Y.; Castellanos, A.; Sabo-Etienne, S.; Chaudret, B. *J. Mol. Catal. A: Chem.* **2004**, *212*, 77−82.

(42) Bolton, P. D.; Grellier, M.; Vautravers, N.; Vendier, L.; Sabo-Etienne, S. *Organometallics* **2008**, *27*, 5088−5093.

(43) Kelley, P.; Lin, S.; Edouard, G.; Day, M. W.; Agapie, T. *J. Am. Chem. Soc.* **2012**, *134*, 5480−5483.

(44) Tobisu, M.; Morioka, T.; Ohtsuki, A.; Chatani, N. *Chem. Sci.* **2015**, *6*, 3410−3414.

(45) Snelgrove, J. L.; Conrad, J. C.; Eelman, M. D.; Moriarty, M. M.; Yap, G. P. A.; Fogg, D. E. *Organometallics* **2005**, *24*, 103−109.

(46) The reaction of $[Ru(H)_2(\eta^2\text{-}H_2)_2(PCy_3)_2]$ with phenol has been reported to form an analogue of **7** (R = H) which converts to **8** (R = H) upon hydrogenation (Scheme 4).[28] Neither of these complexes has been structurally characterized, nor have data been presented to support formation of σ-phenoxide intermediates despite the fact that $[Ru(H)_2(PMe_3)_4]$ reacts with phenol to afford a σ-phenoxide complex *cis*-$[RuH(\kappa^1\text{-}OC_6H_5)(PMe_3)_4]$.[47] Wilkinson and co-workers have commented that $[RuH(PPh_3)_2(\eta^5\text{-}C_6H_5O)\cdot(C_6H_5OH)_2]$ forms a π-phenoxo complex that was reported to crystallize as a 1:2 adduct with phenol; while this finding is directly relevant to our structural characterization of **7a**, the crystallographic data for the former complex is not available in the literature.[89]

(47) Osakada, K.; Ohshiro, K.; Yamamoto, A. *Organometallics* **1991**, *10*, 404−410.

(48) Hartwig, J. F.; Andersen, R. A.; Bergman, R. G. *Organometallics* **1991**, *10*, 1875−1887.

(49) Major, Q.; Lough, A. J.; Gusev, D. G. *Organometallics* **2005**, *24*, 2492−2501.

(50) Camenzind, M. J.; James, B. R.; Dolphin, D.; Sparapany, J. W.; Ibers, J. A. *Inorg. Chem.* **1988**, *27*, 3054−3057.

(51) van der Boom, M. E.; Liou, S.-Y.; Ben-David, Y.; Shimon, L. J. W.; Milstein, D. *J. Am. Chem. Soc.* **1998**, *120*, 6531−6541.

(52) Alós, J.; Esteruelas, M. A.; Oliván, M.; Oñate, E.; Puylaert, P. *Organometallics* **2015**, *34*, 4908−4921.

(53) Perdew, J. P. *Phys. Rev. B: Condens. Matter Mater. Phys.* **1986**, *33*, 8822−8824.

(54) Perdew, J. P. *Phys. Rev. B: Condens. Matter Mater. Phys.* **1986**, *34*, 7406−7406.

(55) Becke, A. D. *Phys. Rev. A: At., Mol., Opt. Phys.* **1988**, *38*, 3098−3100.

(56) Andrae, D.; Huermann, U.; Dolg, M.; Stoll, H.; Preu, H. *Theoret. Chim. Acta* **1990**, *77*, 123−141.

(57) Bergner, A.; Dolg, M.; Küchle, W.; Stoll, H.; Preuß, H. *Mol. Phys.* **1993**, *80*, 1431−1441.

(58) Martin, J. M. L.; Sundermann, A. *J. Chem. Phys.* **2001**, *114*, 3408−3420.

(59) Höllwarth, A.; Böhme, M.; Dapprich, S.; Ehlers, A. W.; Gobbi, A.; Jonas, V.; Köhler, K. F.; Stegmann, R.; Veldkamp, A.; Frenking, G. *Chem. Phys. Lett.* **1993**, *208*, 237−240.

(60) Hehre, W. J.; Ditchfield, R.; Pople, J. A. *J. Chem. Phys.* **1972**, *56*, 2257−2261.

(61) Hariharan, P. C.; Pople, J. A. *Theoret. Chim. Acta* **1973**, *28*, 213−222.

(62) Clark, T.; Chandrasekhar, J.; Spitznagel, G. N. W.; Schleyer, P. V. R. *J. Comput. Chem.* **1983**, *4*, 294−301.

(63) Tomasi, J.; Mennucci, B.; Cammi, R. *Chem. Rev.* **2005**, *105*, 2999−3094.

(64) Grimme, S.; Ehrlich, S.; Goerigk, L. *J. Comput. Chem.* **2011**, *32*, 1456−1465.

(65) Matsubara, T.; Koga, N.; Musaev, D. G.; Morokuma, K. *J. Am. Chem. Soc.* **1998**, *120*, 12692−12693.

(66) Matsubara, T.; Koga, N.; Musaev, D. G.; Morokuma, K. *Organometallics* **2000**, *19*, 2318−2329.

(67) Panetier, J. A.; Macgregor, S. A.; Whittlesey, M. K. *Angew. Chem., Int. Ed.* **2011**, *50*, 2783−2786.

(68) Macgregor, S. A.; McKay, D.; Panetier, J. A.; Whittlesey, M. K. *Dalton Trans.* **2013**, *42*, 7386−7395.

(69) Cybulski, M. K.; McKay, D.; Macgregor, S. A.; Mahon, M. F.; Whittlesey, M. K. *Angew. Chem., Int. Ed.* **2017**, *56*, 1515−1519.

(70) Helmstedt, U.; Clot, E. *Chem. - Eur. J.* **2012**, *18*, 11449−11458.

(71) Perutz, R. N.; Sabo-Etienne, S. *Angew. Chem., Int. Ed.* **2007**, *46*, 2578−2592.

(72) **TS-4** was fully characterized as a transition state on the electronic surface, with IRCs linking it to **Int-4** and **Int-5**. However, **TS-4** fell below these adjacent intermediates upon incorporation of the energy corrections.

(73) Riddlestone, I. M.; Rajabi, N. A.; Lowe, J. P.; Mahon, M. F.; Macgregor, S. A.; Whittlesey, M. K. *J. Am. Chem. Soc.* **2016**, *138*, 11081−11084.

(74) Van Der Sluys, L. S.; Eckert, J.; Eisenstein, O.; Hall, J. H.; Huffman, J. C.; Jackson, S. A.; Koetzle, T. F.; Kubas, G. J.; Vergamini, P. J.; Caulton, K. G. *J. Am. Chem. Soc.* **1990**, *112*, 4831−4841.

(75) Rodriguez, V.; Sabo-Etienne, S.; Chaudret, B.; Thoburn, J.; Ulrich, S.; Limbach, H.-H.; Eckert, J.; Barthelat, J.-C.; Hussein, K.; Marsden, C. J. *Inorg. Chem.* **1998**, *37*, 3475−3485.

(76) This appears to be an effect of the model. The Ru(IV) minimum was not located by Clot and co-workers. Analogous behavior was found in the present study when calculating the intrinsic reaction coordinate from the analogue of **TS-3** with the PCy$_3$ ligands replaced by PMe$_3$, with **Int-4** bypassed with direct formation of **Int-5** (Figure S33).

(77) Grünwald, C.; Gevert, O.; Wolf, J.; González-Herrero, P.; Werner, H. *Organometallics* **1996**, *15*, 1960−1962.

(78) Grellier, M.; Ayed, T.; Barthelat, J.-C.; Albinati, A.; Mason, S.; Vendier, L.; Coppel, Y.; Sabo-Etienne, S. *J. Am. Chem. Soc.* **2009**, *131*, 7633−7640.

(79) Cundari, T. R.; Grimes, T. V.; Gunnoe, T. B. *J. Am. Chem. Soc.* **2007**, *129*, 13172−13182.

(80) Conner, D.; Jayaprakash, K. N.; Cundari, T. R.; Gunnoe, T. B. *Organometallics* **2004**, *23*, 2724−2733.

(81) These include the following: (i) H$_2$ formation accompanied by an intramolecular isomerization of the phosphine ligands, (ii) direct O−H bond formation, and (iii) H$_2$ extrusion followed by β-hydride elimination of a ruthenium-methoxide intermediate (Figures S36 and S37). All three aforementioned pathways are in theory viable as the highest activation barriers of all these pathways are lower than that of the preceding rate-limiting C−O bond cleavage step.

(82) Sieffert, N.; Bühl, M. *J. Am. Chem. Soc.* **2010**, *132*, 8056−8070.

(83) Johansson, A. J.; Zuidema, E.; Bolm, C. *Chem. - Eur. J.* **2010**, *16*, 13487−13499.

(84) Reinhold, M.; McGrady, J. E.; Perutz, R. N. *J. Am. Chem. Soc.* **2004**, *126*, 5268−5276.

(85) Clot, E.; Eisenstein, O.; Jasim, N.; Macgregor, S. A.; McGrady, J. E.; Perutz, R. N. *Acc. Chem. Res.* **2011**, *44*, 333−348.

(86) Hussein, K.; Marsden, C. J.; Barthelat, J.-C.; Rodriguez, V.; Conejero, S.; Sabo-Etienne, S.; Donnadieu, B.; Chaudret, B. *Chem. Commun.* **1999**, 1315−1316.

(87) Delpech, F.; Sabo-Etienne, S.; Daran, J.-C.; Chaudret, B.; Hussein, K.; Marsden, C. J.; Barthelat, J.-C. *J. Am. Chem. Soc.* **1999**, *121*, 6668−6682.

(88) Atheaux, I.; Delpech, F.; Donnadieu, B.; Sabo-Etienne, S.; Chaudret, B.; Hussein, K.; Barthelat, J.-C.; Braun, T.; Duckett, S. B.; Perutz, R. N. *Organometallics* **2002**, *21*, 5347−5357.

(89) Cole-Hamilton, D. J.; Young, R. J.; Wilkinson, G. *J. Chem. Soc., Dalton Trans.* **1976**, 1995−2001.